

Cl⁻ Channels in Basolateral TAL Membranes. XVII. Kinetic Properties of mcCIC-Ka, a Basolateral CTAL Cl⁻ Channel

C.J. Winters, T.E. Andreoli

Division of Nephrology, Department of Internal Medicine, University of Arkansas College of Medicine and The John L. McClellan Veterans Hospital, 4301 West Markham, Slot 640, Little Rock, AR, USA

Received: 10 August 2001/Revised: 5 November 2001

Abstract. This paper describes the kinetics of Cl⁻ flux through mcCIC-Ka Cl⁻ channels from basolateral membranes of mouse CTAL cells. We have cloned two separate but highly homologous Cl⁻ channels, mmCIC-Ka from cultured mouse MTAL cells and mcCIC-Ka from cultured mouse CTAL cells. The mmCIC-Ka and mcCIC-Ka channels appear to mediate net Cl⁻ absorption in the MTAL and CTAL, respectively. The kinetics of Cl⁻ permeation through mmCIC-Ka channels exhibit traditional criteria for a first-order process, including saturation kinetics. Thus mmCIC-Ka channels operate functionally as if the channels were occupied by a single Cl⁻ ion at any given time. In the present studies, we examined conductance-concentration relations in mcCIC-Ka channels, and compared both mole-fraction effects and ion selectivity characteristics in mmCIC-Ka and mcCIC-Ka channels. In mcCIC-Ka channels, we observed both self-block at high external Cl⁻ concentrations and, at constant ionic strength, an anomalous mole-fraction effect using external solutions containing varying F⁻/Cl⁻ concentrations. Neither effect was obtained in mmCIC-Ka channels. These data are consistent with the possibility that Cl⁻ permeation through mcCIC-Ka channels involved multi-ion occupancy channels that expressed single-file behavior.

Key words: Cl⁻ channels — Multi-ion occupancy — CTAL — Self-block — Anion selectivity — Anomalous mole fraction effect

Introduction

This paper describes the kinetics of Cl⁻ flux through mcCIC-Ka Cl⁻ channels from basolateral membranes of mouse CTAL cells [21, 23]. We have cloned two separate but highly homologous Cl⁻ channels, mmCIC-Ka from cultured mouse MTAL cells and mcCIC-Ka from cultured mouse CTAL cells [23]. mmCIC-Ka appears to be the mouse homologue to rat CIC-K2 [1, 16], to human CIC-Kb [7] and to rabbit rbCIC-Ka [23, 25], while mcCIC-Ka shares high homology with rCIC-K1 [16] present in thin ascending limbs. Moreover, anti-rbCIC-Ka, a polyclonal antibody to rbCIC-Ka [20], also reacts with mmCIC-Ka [20] and mcCIC-Ka [21].

Despite the high sequence homology [23] between mmCIC-Ka and mcCIC-Ka, the physiologic characteristics of these two channels differ appreciably [21]. The mmCIC-Ka channel is gated, without (ATP + PKA), by increases in cytosolic Cl⁻ concentrations in the range 2–25 mM ($K_{1/2} = 10$ mM) [19, 21]. At low cytosolic Cl⁻ concentrations, 2 mM, (ATP + PKA) also gate mmCIC-Ka channels [19, 21], but at normal physiologic cytosolic Cl⁻ concentrations, 25 mM [10], (ATP + PKA) have no effect on the open-time probability of mmCIC-Ka [19, 21]. These properties, unique to our knowledge among the CIC family of Cl⁻ channels [4], are entirely absent in mcCIC-Ka channels [21]. And as described previously [9, 21, 23], our experimental data are consistent with the view that, so far as net Cl⁻ absorption is concerned, the process is mediated functionally by mmCIC-Ka in MTAL cells and by mcCIC-Ka in CTAL cells.

Of particular pertinence to the present studies, an analysis [22] of the kinetics of Cl⁻ permeation through mmCIC-Ka channels indicated that these channels exhibited the traditional criteria [5, 8, 13] for a first-order

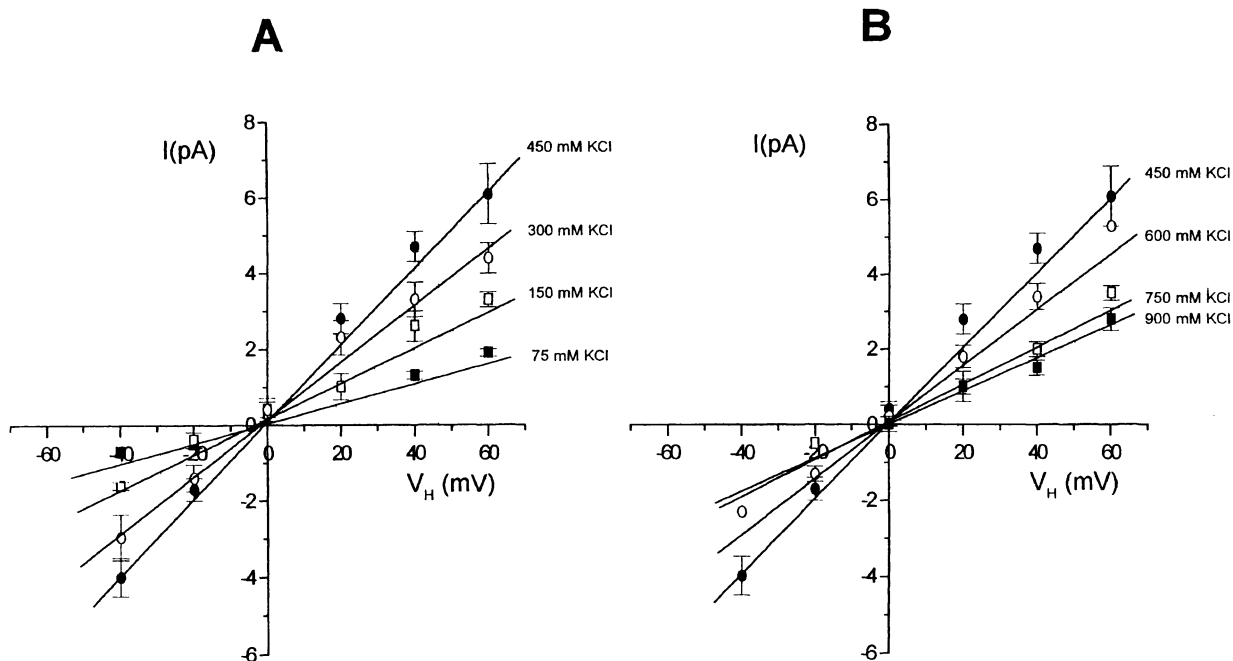


Fig. 1. Current-voltage relations using seven different symmetrical solutions. All data were fitted by linear regression. (A) Symmetrical KCl: 75 mM ($n = 3$, $r = 0.96$), 150 mM ($n = 7$, $r = 0.98$), 300 mM ($n = 22$, $r = 0.99$) and 450 mM ($n = 12$, $r = 0.99$); (B) Symmetrical KCl: 450 mM ($n = 12$, $r = 0.99$), 600 mM ($n = 9$, $r = 0.98$), 750 mM ($n = 4$, $r = 0.97$) and 900 mM ($n = 4$, $r = 0.97$).

process, including saturation kinetics, that could be rationalized quantitatively by the Michaelis expression applied to conductance-concentration relations with a $K_{1/2} = 163$ mM Cl. Put differently, mmClC-Ka channels operate functionally as if the channels were occupied by a single Cl^- ion at any given time.

In the present studies, we examined conductance-concentration relations in mcClC-Ka channels, and compared both mole-fraction [5] effects and ion selectivity characteristics in mmClC-Ka and mcClC-Ka channels. In mcClC-Ka channels, we observed both self-block at high external Cl^- concentrations and, at constant ionic strength, an anomalous mole-fraction effect using external solutions containing varying F^-/Cl^- concentrations. Neither effect obtained in mmClC-Ka channels. A kinetic analysis of these data indicated that Cl^- permeation through mcClC-Ka channels was consistent with the possibility that the latter were multi-ion occupancy channels [5, 13] that expressed single-file kinetics of the type originally described by Hodgkin and Keynes [6].

A preliminary report of these findings has appeared in abstract form [24].

Materials and Methods

The procedures for preparing and isolating basolaterally enriched vesicles from cultured mouse CTAL and MTAL cells have been described previously [18, 20]. For the present studies, these vesicles were suspended in 250 mM sucrose and 30 mM histidine (pH 7.4) at a protein concentration of 10–20 mg/ml.

Lipid bilayer membranes were formed as described previously [14, 19–21]. The solutions used to form bilayers were a 1:1 mixture of phosphatidylserine and phosphatidylethanolamine in decane (20 mg lipid/ml). The bilayers were voltage clamped using a patch-clamp amplifier (Dagan 8900, Minneapolis, MN) connected to the bilayer chambers via silver electrodes in 3 mM KCl agar bridges. Records were stored and analyzed by computer using pclamp 5.5 (Axon Instruments, Foster City, CA). Records were filtered at 200 Hz (-3 dB cutoff) and sampled at 2 kHz. All voltages reported in this paper are expressed for *trans* solutions with respect to *cis* solutions.

Basolateral vesicles from cultured mouse CTAL cells were used to obtain mcClC-Ka channels [18, 20], and basolateral vesicles from cultured mouse MTAL cells were used to obtain mmClC-Ka channels [20, 21, 23]. The methods for vesicle incorporation into lipid bilayers were used as described previously [14, 19–21, 23]. In the present studies, *cis* and *trans* chambers uniformly contained 1 mM CaCl_2 and 5 mM HEPES, pH 7.4. The KCl concentrations in the *cis* and *trans* solutions in each experiment are indicated in the Results. KF, KI and KIsethionate (KIse) were added directly from a stock 3 M solution. Openings and closings of the channel were defined by a 50% threshold discriminator. All results were expressed as mean values \pm SEM for the indicated number of experiments. A single bilayer was taken to be $n = 1$. Curve fitting and simple linear regression were done on computer using "Origin 4.1" (Microcal Software, Northampton, MA).

Results

CURRENT-VOLTAGE RELATIONS

Figure 1 shows the current/voltage (I/V) relations of these mcClC-Ka channels for symmetrical *cis* and

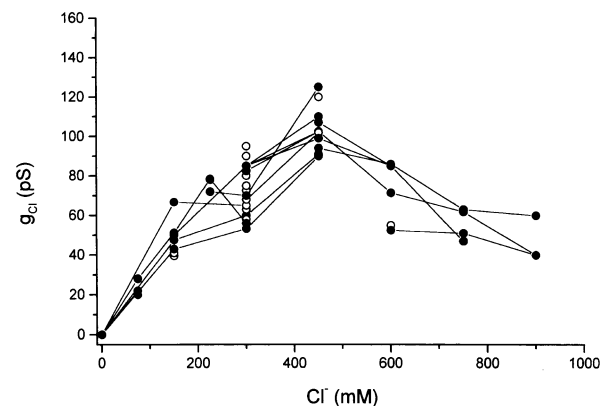


Fig. 2. The relation between the slope conductance g_{Cl} and varying symmetrical Cl^- concentrations measured in the 55 bilayer experiments illustrated in Fig. 1. Closed circles and lines connect paired experiments; the open circles are unpaired experiments.

trans KCl concentrations in the range 75–900 mM. Figure 1A shows that, for external concentrations in the range 75–450 mM, the I/V relations were linear at each of the KCl concentrations tested. Moreover, for the four KCl concentrations tested, the slopes of the I/V relations, that is, g_{Cl} (pS), were positive linear functions of external KCl concentrations. Figure 1B shows that, for each of the four KCl concentrations tested — 450, 600, 750, and 900 mM — we also observed linear I/V relations. However, at external KCl concentrations in excess of 450 mM, g_{Cl} fell as external KCl concentrations rose.

Figures 2 and 3 illustrate these data quantitatively by plotting g_{Cl} as a function of external Cl^- concentrations. At KCl concentrations exceeding 450 mM, there occurred self-block characteristic of channels having single-file behavior with simultaneous multiple ion occupancy [5, 8, 13]. Clearly, using predominantly paired measurements, g_{Cl} fell linearly when external KCl concentrations exceeded 450 mM.

Figure 3 compares the data (mean \pm SEM) from Fig. 2, using mmClC-Ka channels, with the data reported previously [22] for mmClC-Ka channels. The dashed lines in Fig. 3 are from Fig. 2 in Ref. 22 for mmClC-Ka channels. Even at external Cl^- concentrations well in excess of 600 mM, mmClC-Ka channels exhibited classical saturation kinetics typical of channels containing a single ion, in this case Cl^- , at any given time [5, 8, 13].

ANION SELECTIVITY

We evaluated the anion selectivity sequence for these mmClC-Ka channels using a protocol identical to that used for evaluating anion selectivity patterns in rabbit rbClC-Ka channels [18]. Specifically, the *cis* solutions contained 300 mM KCl and the *trans* solutions contained 50 mM KCl plus 250 mM K^+ salts of the various test anions. Under these conditions we

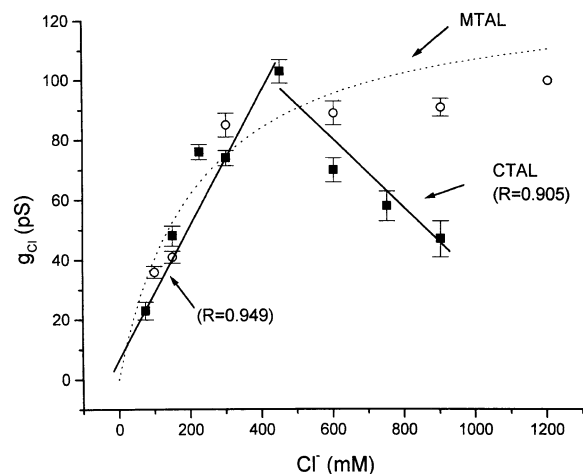


Fig. 3. Mean values \pm SEM published previously [22] for mmClC-Ka channels fitted by the Michaelis expression ($R_2 = 0.986$; $G_{Cl}^{max} = 114$ pS; $K_{1/2} = 163$ mM Cl^- (open circles). Mean values \pm SEM for all the data presented in Fig. 2. The solid lines indicate the positive linear slope for Cl^- concentrations in the range 0–450 mM and the negative linear slope for Cl^- concentrations in the range 450–900 mM (closed circles).

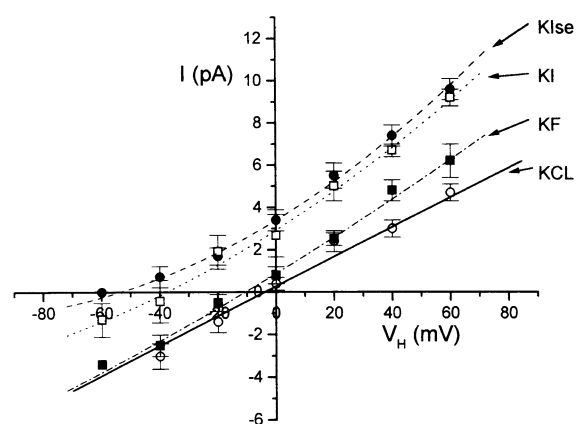


Fig. 4. Evaluation of anion selectivity. Current-voltage (I/V) relations were carried out when *cis* solutions contained 300 mM KCl and the *trans* solutions contained 50 mM KCl plus 250 mM of the K^+ salt of each of the indicated anions. The results are expressed as mean values for the number of bilayers indicated for each test anion in Table 1.

measured both I/V relations and zero-current reversal voltages (V_r , mV).

The results shown in Fig. 4 indicate that, in accord with the data presented in Fig. 1, the I/V relations were linear for KCl in the range ± 60 mV and, for the other anions, virtually linear in the range ± 40 mV. Table 1 shows the zero-current reversal voltages for isethionate, I^- and F^- with respect to Cl^- . The ionic selectivity sequence observed, $F^-/Cl^- = 0.67$, $I^-/Cl^- = 0.13$ and $Ise^-/Cl^- = 0.08$, was qualitatively the same as that observed previously [18] by us for rbClC-Ka channels from rabbit outer medulla.

Table 1. Anion selectivity of mcCIC-Ka CTAL Cl⁻ channels

Anion	V_r (mV)	N	P_x/P_{Cl}
F ⁻	-9.9 ± 2.8	3	0.67
I ⁻	-36.1 ± 4.7	4	0.13
Ise ⁻	-51.5 ± 3.8	7	0.08

The V_r data are from the experiments illustrated in Fig. 4. V_r was measured when the *cis* chamber contained 300 mM KCl and the *trans* chamber contained 50 mM KCl and 250 mM of the K⁺ salt of the indicated anion. The results are expressed as mean values \pm SEM for the indicated number of bilayers.

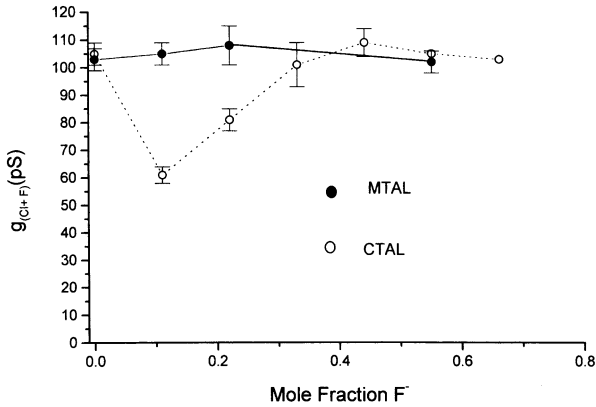


Fig. 5. Effect of raising *cis* F⁻ anion mole fraction on total single-channel conductance $g_{(Cl+F)}$ in mmCIC-Ka (closed circles) and mcCIC-Ka (open circles) Cl⁻ channels from CTAL and MTAL cells, respectively. The *cis* solutions contained total 450 mM K⁺ salts of Cl⁻ and F⁻ at the indicated mole fractions for F⁻. The *trans* solutions contained 450 mM KCl. The single-channel conductances were measured between ± 60 mV, and the results are expressed as mean values \pm SEM.

ANOMALOUS MOLE-FRACTION EFFECT

The anomalous mole-fraction effect, in phenomenologic terms, involves channel conductances passing through a minimum when different mole fractions of one permeant anion are substituted for another permeant anion, all at constant ionic strength. This effect is generally [5, 8, 13, 15] but not universally [12] considered to be the consequence of channels holding at least two ions at the same time.

The data presented in Fig. 5 and Table 2 evaluated the possibility of an anomalous mole fraction effect in both mmCIC-Ka channels and mcCIC-Ka channels. In both sets of experiments, the *trans* solutions contained 450 mM KCl and the *cis* solutions varying mole fractions of F⁻, with total *cis* anion concentrations (Cl⁻ + F⁻) of 450 mM. The F⁻ anion was used since, from Table 1, the F⁻/Cl⁻ selectivity ratio was the highest among the anions tested.

The data shown in Fig. 5 indicate explicitly that, for mmCIC-Ka channels, $g_{(Cl+F)}$, the total single channel conductance, remained virtually constant for F⁻/Cl⁻ mole fractions in the range 0–0.6. The data

Table 2. Comparison of mcCIC-Ka Cl⁻ channel conductances at different extracellular F⁻ mole fractions

F ⁻ mole fraction	$g_{(Cl+F)}$ (S)	N	p
0	105 ± 4	16	–
0.11	61 ± 3	7	0.00001
0.22	81 ± 4	3	0.007
0.33	101 ± 8	4	NS
0.44	109 ± 5	3	NS

The data are from Fig. 5. The values of g_{Cl} are expressed as mean values \pm SEM for the indicated number of bilayers.

presented in Fig. 5 also show that, for mcCIC-Ka channels, $g_{(Cl+F)}$ went through a distinct minimum at an F⁻/Cl⁻ mole fraction of 0.1, and returned to control values at an F⁻/Cl⁻ mole fraction slightly in excess of 0.3. These latter data are illustrated quantitatively in Table 2. At an F⁻/Cl⁻ mole fraction of 0.11, $g_{(Cl+F)}$ fell from a control value of 101 ± 4 pS to 61.3 ± 3 pS ($p = 10^{-5}$), rose to 81 ± 4 pS ($p = 0.007$) at a mole fraction of 0.22, and returned to control values of 101 ± 8 pS at an F⁻/Cl⁻ mole fraction of 0.33.

Discussion

The experiments reported in this paper describe yet another example of functional heterogeneity between mmCIC-Ka and mcCIC-Ka channels, that is, strikingly different kinetic properties for ionic conductance through the two channels. We now consider these differences in detail.

In kinetic terms, mmCIC-Ka channels exhibit first-order saturation kinetics with a $K_{1/2}$ of 163 mM and a G_{Cl}^{max} of 114 pS ([22]; Fig. 3). To illustrate this point in more detail, Fig. 6 shows the latter data plotted according to the Eadie-Hofstee relation [11]:

$$g_{Cl} = (-K_{1/2})g_{Cl}/[Cl^-] + G_{Cl}^{max} \quad (1)$$

The lower half of Fig. 6 show that, by using equation 1 for MTAL channels, we obtained a linear relation ($R = 0.75$). From the slope and intercept, we obtain a $K_{1/2}$ of 156 mM Cl⁻ and a G_{Cl}^{max} of 112 pS, respectively. In short, the $K_{1/2}$ and G_{Cl}^{max} values for mmCIC-Ka channels were virtually the same when analyzed according to the Michaelis expression (Fig. 3) or an Eadie-Hofstee plot (Fig. 6).

We also evaluated the MTAL data according to a form of the Hill equation [8]:

$$\log(g_{Cl}/G_{Cl}^{max} - g_{Cl}) = N \log[Cl^-] - \log N' \quad (2)$$

where N is the slope and N' is a complex zero-intercept constant referring, in part, to the cooperativity of ion conductance [5, 8, 17]. The relevant observation, shown in the lower half of Fig. 7, is that for MTAL channels using a G_{Cl}^{max} of 112 pS (Fig. 6), we obtained a slope of 1.01 for mmCIC-Ka channels.

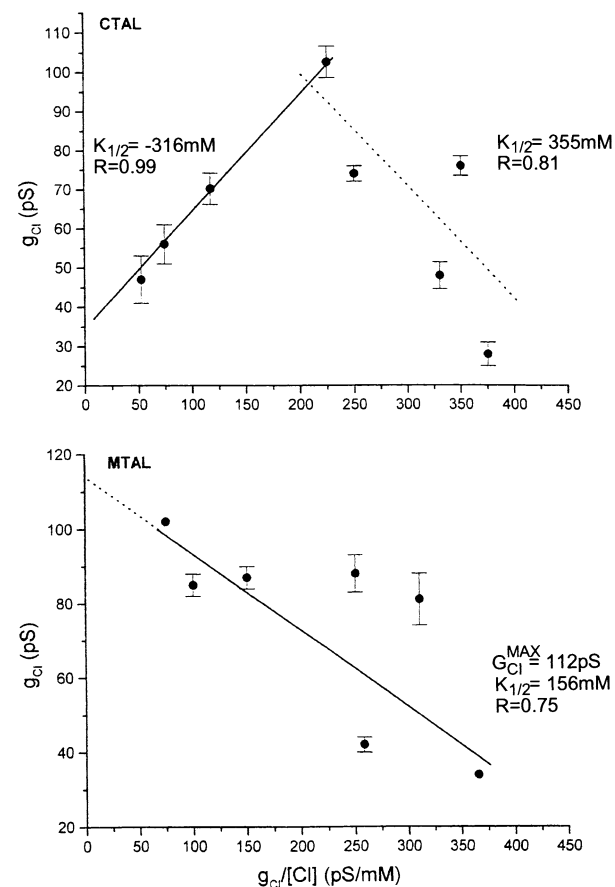


Fig. 6. Eadie-Hofstee plots of the relation between g_{Cl} and $g_{\text{Cl}}/[\text{Cl}^-]$ with $[\text{Cl}^-]$ representing the KCl concentrations in symmetrical external solutions. The data for mcCIC-Ka channels from CTAL cells are from Figs. 2 and 3. No $G_{\text{Cl}}^{\text{max}}$ could be calculated from the slope of g_{Cl} with respect to $g/[\text{Cl}^-]$ since the slope was positive at $g/[\text{Cl}^-]$ values less than 225 pS/mM and negative for $g/[\text{Cl}^-]$ values greater than 225 pS/mM. Thus for $G_{\text{Cl}}^{\text{max}}$ for mcCIC-Ka channels in the Hill plots shown in Fig. 7, we used the highest g_{Cl} observed experimentally in Fig. 2, that is, 115 pS. The g_{Cl} data for mmCIC-Ka channels are those published previously (Fig. 2 in Ref. [22]) and shown in Figs. 3 and 6.

Moreover, as indicated in Fig. 5, no anomalous mole-fraction effect was observed in mmCIC-Ka channels. Thus when taken together, the results presented in Figs. 3, 6 and 7 provide added support to our earlier contention [22] that Cl⁻ conductance through mmCIC-Ka channels occurs by channel occupancy by a single Cl⁻ ion at any given time [5, 8, 13, 22].

The anion selectivity sequences (Fig. 4; Table 1) for mcCIC-Ka channels were qualitatively similar to those observed in mmCIC-Ka channels [18]. However, the kinetic behavior of mcCIC-Ka channels differed strikingly from that observed in mmCIC-Ka channels (Figs. 1, 2, 3, 6, 7). First, as indicated clearly in Figs. 1–3, g_{Cl} in mcCIC-Ka channels declined sharply when external Cl⁻ concentrations exceeded 450 mM. Fig. 6 indicates that the Eadie-Hofstee plots for mcCIC-Ka channels were qualitatively different

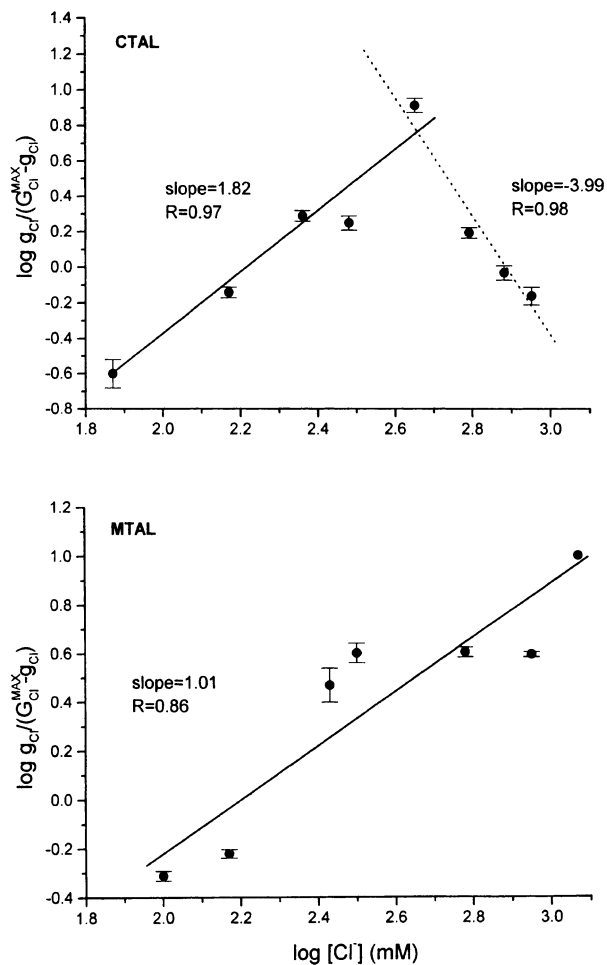


Fig. 7. Hill plots of $\log g_{\text{Cl}}/(G_{\text{Cl}}^{\text{max}} - g_{\text{Cl}})$ with respect to $\log [\text{Cl}^-]$ fusing the results presented in Fig. 6.

from the results obtained with mmCIC-Ka channels. More specifically, the upper panel of Fig. 6 indicates that we observed a positive slope of the relation between g_{Cl} and $g_{\text{Cl}}/[\text{Cl}^-]$ at $g_{\text{Cl}}/[\text{Cl}^-]$ values less than 200 pS/mM, and a negative slope at $g_{\text{Cl}}/[\text{Cl}^-]$ values greater than 200 pS/mM. Second, in mmCIC-Ka channels, Hill plots of $\log g_{\text{Cl}}/(G_{\text{Cl}}^{\text{max}} - g_{\text{Cl}})$ yielded, for $\log [\text{Cl}^-]$ concentrations in the range 2.0–3.1, a positive linear relation with a unity slope (lower half of Fig. 7). In contrast, in Hill plots using the conductance-concentration relations for mcCIC-Ka channels reported in Fig. 3, we observed (upper half of Fig. 7): with $\log [\text{Cl}^-]$ concentrations in the range 1.9–2.6, a positive linear relation with a slope of 1.82, and for $\log [\text{Cl}^-]$ concentrations in the range 2.6–3.0, a negative linear relation with a slope of -3.99. The latter differed significantly from 1.82, the positive linear slope observed in mcCIC-Ka channels with $\log [\text{Cl}^-]$ concentrations in the range 1.9–2.6.

This self-block observed with mcCIC-Ka channels (Figs. 1, 2, 3, 6, 7) is unique, to our knowledge, among CIC channels, including CIC-0 and other CIC

channels presumed to have double-barreled channel architecture [2–4]. We interpret the results presented in Figs. 1, 3, 6 and 7, together with the anomalous mole-fraction data presented in Fig. 5 and Table 2, to indicate that these mcClC-Ka channels contain multiple ions simultaneously, and that the functional geometry of these channels precludes side-by-side passage of Cl⁻ ions [5, 8, 11, 13, 15, 17].

We have no insight into the factors governing the strikingly different kinetic behavior of mmClC-Ka channels and mcClC-Ka channels, a surprising finding given the 95% identity between the amino-acid sequences of the two channels [23]. However, it should be noted in this context that the mmClC-Ka and mcClC-Ka channels were incorporated into bilayers using basolateral vesicles from mmClC-Ka and mcClC-Ka cells, respectively. And the Cl⁻ transport properties of MTAL and CTAL cells are quite different (22), as are many of the transport properties of mmClC-Ka and mcClC-Ka channels (see Introduction). Thus it may be that the differing microenvironments of mmClC-Ka and mcClC-Ka channels may play a role in modulating the different kinetic conductance properties of the mmClC-Ka and mcClC-Ka channels. Obviously, added experimental data will be required to evaluate this possibility, or alternative explanations.

We are grateful for the technical assistance provided by Ms. Anna Grace Stewart and for assistance in preparing this manuscript provided by Ms. Clementine M. Whitman. This work was supported by NIH Grant 5 R01 DK25540 to T. E. Andreoli.

References

- Adachi, S., Uchida, S., Ito, H., Hata, M., Hiroe, M., Marumo, F., Sasaki, 1994. Two isoforms of a chloride predominantly expressed in thick ascending limb of Henle's loop and collecting ducts of rat kidney. *J. Biol. Chem.* **269**:17677–17683
- Fahlke, C., Yu, H.T., Beck, C.L., Rhodes, T.H., George, A.L., Jr. 1997. Pore-forming segments in voltage-gated chloride channels. *Nature* **390**:529–532
- Fahlke, C., Rhodes, T.H., Desai, R.R., George, A.L., Jr. 1998. Pore stoichiometry of a voltage-gated chloride channel. *Nature* **394**:687–690
- Fahlke, C. 2001. Ion permeation and selectivity in ClC-type chloride channels. *Am. J. Physiol.* **280**:F748–F757
- Hille, B. 1992. Selective permeability: Saturation and binding. *In: Ionic Channels of Excitable Membranes*, pp. 362–389. Sinauer Associates, MA, Sunderland
- Hodgkin, A.L., Keynes, R.D. 1955. The potassium permeability of a giant nerve fibre. *J. Physiol.* **128**:61–88
- Kieferle, S., Fong, P., Bens, M., Vandewalle, A., Jentsch, T.J. 1994. Two highly homologous members of the ClC chloride channel family in both rat and human kidney. *Proc. Nat. Acad. Sci. USA.* **91**:6943–6947
- Läuger, P. 1987. Dynamics of ion transport systems in membranes. *Physiol. Rev.* **67**:1196–1331
- Mikhailova, M.V., Winters, C.J., Andreoli, T.E. 2001. Quantitative determination of mmClC and mcClC chloride channel expression in mouse kidney. *J. Am. Soc. Neph.* **12**:36A–37A
- Molony, D.A., Reeves, W.B., Hebert, S.C., Andreoli, T.E. 1987. ADH increases apical Na⁺, K⁺, 2Cl⁻ entry in mouse medullary thick ascending limbs of Henle. *Am. J. Physiol.* **252**:F177–F187
- Neher, E., Sandblom, J., Eisenman, G. 1978. Ionic Selectivity, saturation and block in gramicidin A channels. II. Saturation behavior of single channel conductances and evidence for the existence of multiple binding sites in the channel. *J. Membrane Biol.* **40**:97–116
- Nonner, W., Chen, D.P., Eisenberg, B. 1998. Anomalous mole fraction effect, electrostatics, and binding in ionic channels. *Biophys. J.* **74**:2327–2334
- Pappone, P.A., Cahalan, M.D. 1986. Ion permeation in cell membranes. *In: Physiology of Membrane Disorders*. Second Edition. T.E. Andreoli, J.F. Hoffman, D.D. Fanestil, S.G. Schultz, Editors, pp. 249–272. Plenum Publishing, New York
- Reeves, W.B., Winters, C.J., Filipovic, D.M., Andreoli, T.E. 1995. Cl⁻ channels in basolateral renal medullary vesicles. IX. Channels from mouse mTAL cell patches and medullary vesicles. *Am. J. Physiology: Renal Fluid and Electrolyte Physiol.* **269**:F621–F627
- Sandblom, J., Eisenman, G., Neher, E. 1977. Ionic selectivity, saturation and block in gramicidin A channels: I. Theory for the electrical properties of ion selective channels having two pairs of binding sites and multiple conductance states. *J. Membrane Biol.* **31**:383–417
- Uchida, S. 2000. *In vivo* role of ClC chloride channels in the kidney. *Am. J. Physiol.* **279**:F802–F808
- Urban, B.W., Hladky, S.B., Haydon, D.A. 1978. The kinetics of ion movements in the gramicidin channel. *Fed. Proc.* **37**:2628–2632
- Winters, C.J., Reeves, W.B., Andreoli, T.E. 1990. Cl⁻ channels in basolateral renal medullary membranes. III. Determinants of single channel activity. *J. Membrane Biol.* **118**:269–278
- Winters, C.J., Reeves, W.B., Andreoli, T.E. 1991. Cl⁻ channels in basolateral renal medullary membrane vesicles. IV. Interactions of Cl⁻ and cAMP-dependent protein kinase with channel-activity. *J. Membrane Biol.* **122**:89–95
- Winters, C.J., Zimniak, L., Reeves, W.B., Andreoli, T.E. 1997. Cl⁻ channels in basolateral renal medullary membranes. XII. Anti-rbClC-Ka antibody blocks mTAL Cl⁻ channels. *Am. J. Physiol.* **273**:F1030–F1038
- Winters, C.J., Reeves, W.B., Andreoli, T.E. 1999. Cl⁻ channels in basolateral TAL membranes: XIII. Heterogeneity between basolateral MTAL and CTAL Cl⁻ channels. *Kidney Internat.* **55**:593–601
- Winters, C.J., Reeves, W.B., Andreoli, T.E. 1999. Cl⁻ channels in basolateral TAL membranes: XIV. Kinetic properties of a basolateral MTAL Cl⁻ channel. *Kidney Internat.* **55**:1444–1449
- Winters, C.J., Zimniak, L., Mikhailova, M.V., Reeves, W.B., Andreoli, T.E. 2000. Cl⁻ channels in basolateral TAL membranes: XV. Molecular heterogeneity between cortical and medullary channels. *J. Membrane Biol.* **177**:221–230
- Winters, C.J., Andreoli, T.E. 2001. Kinetic properties of basolateral cortical thick ascending (CTAL) Cl⁻ channels. *J. Am. Soc. Neph.* **12**:43A–44A
- Zimniak, L., Winters, C. J., Reeves, W. B., Andreoli, T. E. 1995. Cl⁻ channels in basolateral renal medullary vesicles. X. Cloning of a Cl⁻ channel from rabbit outer medulla. *Kidney Internat.* **48**:1828–1836